inorganics

MDPI

Article

Probing the Effect of Six-Membered *N*-Heterocyclic Carbene—6-Mes—on the Synthesis, Structure and Reactivity of $Me_2MOR(NHC)$ (M = Ga, In) Complexes

Martyna Cybularczyk-Cecotka [1,2], Anna Maria Dąbrowska [1,3], Piotr A. Guńka [3] and Paweł Horeglad [1,*]

1 Centre of New Technologies, University of Warsaw, Banacha 2c, 02-097 Warsaw, Poland; m_cybularczyk@wp.pl (M.C.-C.); a.dabrowska@cent.uw.edu.pl (A.M.D.)
2 Faculty of Chemistry, University of Warsaw, Pasteura 1, 02-093 Warsaw, Poland
3 Faculty of Chemistry, Warsaw University of Technology, Noakowskiego 3, 00-664 Warsaw, Poland; piogun@ch.pw.edu.pl
* Correspondence: p.horeglad@cent.uw.edu.pl; Tel.: +48-22-5543670

Received: 3 January 2018; Accepted: 12 February 2018; Published: 16 February 2018

Abstract: The investigation of the reactivity of six membered *N*-heterocyclic carbene 1,3-bis(2,4,6-trimethylphenyl)-3,4,5,6-tetrahydropyrimidin-1-ylidene (6-Mes) towards dialkylgallium and dialkylindium alkoxides/aryloxides has shown that both steric hindrances and donor properties of 6-Mes significantly influence the strength of $M–C_{6\text{-Mes}}$ bond, as well as the formation, structure and reactivity of $Me_2MOR(6\text{-Mes})$ (M = Ga, In) complexes. While the reactions of simple dimethylgallium alkoxides with 6-Mes lead to the formation of stable monomeric $Me_2Ga(OCH_2CH_2OMe)(6\text{-Mes})$ (**1**) and $Me_2GaOMe(6\text{-Mes})$ complexes, the analogous $Me_2InOR(6\text{-Mes})$ are unstable and disproportionate to methylindium alkoxides and $Me_3In(6\text{-Mes})$ (**2**). The use of bulky alkoxide ligand—$OCPh_2Me$ or aryloxide ligand—OC_6H_4OMe allowed for the synthesis of stable $Me_2M(OCPh_2Me)(6\text{-Mes})$ (M = Ga (**3**) and In (**4**)) as well as $Me_2M(OC_6H_4OMe)(6\text{-Mes})$ (M = Ga (**5**) and In (**6**)). The structures of **1**–**6** have been determined using both spectroscopic methods in solution and X-ray diffraction studies, which confirmed the effect of both steric hindrances and donor properties of 6-Mes on their structure and catalytic properties in the ring-opening polymerization (ROP) of *rac*-lactide.

Keywords: metal alkoxides; main group metals; NHC donor strength; catalyst; lactide; stereoselectivity; isotactic polylactide

1. Introduction

Over recent years, we have reported $Me_2MOR(NHC)$ (M = Ga [1,2], In [3]; NHC = *N*-heterocyclic carbene) complexes, which constitute the first examples of gallium and indium, as well as group 13 metal alkoxides, with NHCs [4]. Moreover, they represent isoselective catalysts for the ring-opening polymerization (ROP) of *rac*-lactide (*rac*-LA), which are additionally highly active at low temperatures. Therefore, they still constitute rare examples of isoselective catalysts operating at mild conditions, both among group 13 metal complexes [5–9], and beyond [10–13]. Importantly, both the structure and reactivity of $Me_2MOR(NHC)$ (M = Ga, In; NHC = SIMes, IMes) were found to be strongly dependent on the $M–C_{NHC}$ bond. While in the case of corresponding gallium complexes, a relatively strong $Ga–C_{NHC}$ bond led to stable complexes [1,2], in the case of mostly unstable dialkylindium alkoxides with NHCs, a significantly weaker $In–C_{NHC}$ bond was observed [3]. Consequently, in the ring-opening polymerization with $Me_2GaOR(NHC)$, $Ga–C_{NHC}$ bond remained intact, resulting in the exclusive insertion of *rac*-LA into $Ga–O_{alkoxide}$ bond, similar to Zn [14–16], Al [17], as well as Ti and Zr [18–20], metal alkoxides with NHCs, which have been reported to polymerize *rac*-LA due to the insertion into

M–$O_{alkoxide}$ bond. On the other hand, *rac*-LA could insert, even at low temperature, into In–C_{NHC} bond of Me_2GaOR(NHC), considerably weaker in comparison with Ga–C_{NHC} [3]. Analogously, the insertion of lactide into the M–C_{NHC} bond of Mg alkoxides with alkoxide ligands possessing NHC termini [16], Me_3Al(NHC) adducts [21], or yttrium and titanium complexes [22], have been reported so far.

Similarly to the observed effect of a metal on the corresponding M–C_{NHC} bond, as well as the structure and ROP activity of discussed main group metal alkoxides with NHCs, we should expect a considerable effect of steric and electronic properties of NHC on both the strength and reactivity of the M–C_{NHC} bond. Our initial studies revealed the adverse effect of steric hindrances of NHC on the synthesis of Me_2GaOR(SIPr) as well as the formation and strength of Ga–C_{SIPr} bond [2], which was additionally supported by the structure of Me_3M(NHC) (M = Al, Ga, In) adducts [3,21,23]. However, the more detailed effect of both steric and electronic effect of NHC on the M–C_{NHC} bond has not been addressed so far for main group metal alkoxides with NHCs, including Me_2MOR(NHC) (M = Ga, In) complexes. In order to probe the effect of NHC on the latter, we chose 6-Mes—an *N*-heterocyclic carbene of stronger donor properties, along with the increased steric demand, in comparison with SIMes or IMes (Figure 1) [24,25]. While the increased steric hindrances of 6-Mes result from wider N–C–N angle, this should be responsible for the hybridization at carbene carbon and the higher energy of HOMO orbital of 6-Mes occupied by a lone pair of electrons, and therefore its donating properties [26].

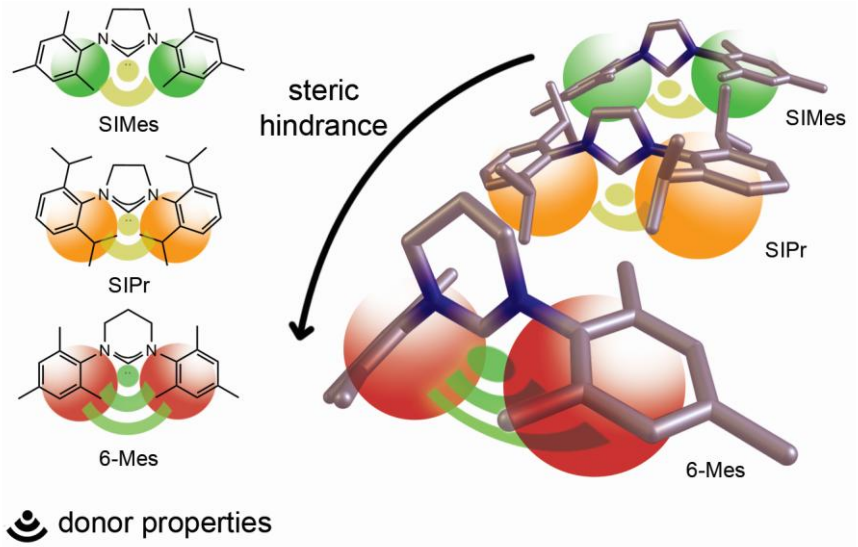

Figure 1. Relationship between steric and electronic properties of 6-Mes and SIMes/SIPr —previously used for the synthesis of Me_2MOR(NHC) (M = Ga, In) complexes [1–3].

Our studies, reported hereby, have allowed for the determination of the considerable effect of steric and electronic properties of 6-Mes, as well as the relative importance of electronic and steric properties of 6-Mes, on the synthesis, structure and stability of a series of Me_2MOR(NHC) (M = Ga, In) complexes, as well as their catalytic activity in the ROP of *rac*-LA.

2. Results and Discussion

In order to observe the influence of steric and electronic properties NHC on the synthesis, structure and reactivity of Me_2MOR(NHC) (M = Ga, In) complexes, we investigated the reactivity of dimethylgallium and dimethylindium alkoxides and aryloxides towards 1,3-bis(2,4,6-trimethylphenyl)-3,4,5,6-tetrahydropyrimidin-1-ylidene (6-Mes). The synthesis, structure of resulting Me_2MOR(6-Mes) (M = Ga, In) complexes, and their catalytic activity in the ROP of *rac*-LA was compared to the analogous dialkylgallium and dialkylindium derivatives stabilized with 1,3-bis(2,4,6-trimethylphenyl)imidazolin-2-ylidene (SIMes) or 1,3-bis(2,4,6-trimethylphenyl) imidazolin-2-ylidene (IMes) [1–3].

2.1. Reactivity of $[Me_2M(\mu\text{-}OR)]_n$ (M= Ga, In ; OR = OCH_2CH_2OMe, OMe ; n = 2, 3) towards 6-Mes

The reaction between dimeric gallium complex $[Me_2Ga(\mu\text{-}OCH_2CH_2OMe)]_2$ and 6-Mes (Ga:6-Mes = 1:1, Scheme 1) led to the essentially instant formation of gallium complex $Me_2Ga(OCH_2CH_2OMe)$(6-Mes) (**1**). Compound **1** was isolated as an off-white solid in high yield. Unfortunately, the crystals of **1** decomposed during an X-ray diffraction experiment, which precluded the determination of its X-ray structure. Notably, the increased reactivity of **1** towards grease during X-ray experiment, in comparison with Me_2GaOR(NHC) (NHC = SIMes, IMes), should not be surprising in the light of its structure and reactivity in solution.

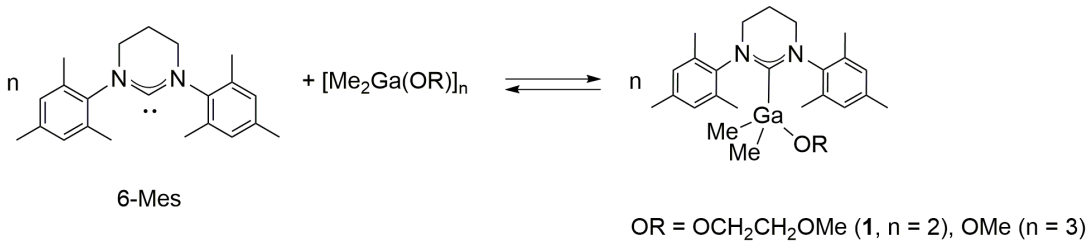

Scheme 1. Synthesis of Me_2GaOR(6-Mes) complexes.

In solution, both ^{1}H NMR, and ^{13}C NMR were indicative of the formation of **1**. Although two sets of signals were revealed by ^{1}H NMR of **1** in toluene-d_8, the main set of signals, including a singlet corresponding to Ga–Me protons (−1.06 ppm), which was significantly shifted to higher field, similarly to $Me_2Ga(OCH_2CH_2OMe)$(SIMes) [2], was indicative of the formation of $Me_2Ga(OCH_2CH_2OMe)$(6-Mes). The additional minor set of signals corresponded to $[Me_2Ga(OCH_2CH_2OMe)]_2$ (16%), which suggested the presence of an equilibrium, presented in Scheme 1. Such an equilibrium was further evidenced by a 2D ROESY (rotating frame Overhauser effect spectroscopy) experiment (Figure S3). Moreover, essentially the same ratio of $Me_2Ga(OCH_2CH_2OMe)$(6-Mes): $[Me_2Ga(OCH_2CH_2OMe)]_2$, for **1**, and the reaction mixture of $[Me_2Ga(\mu\text{-}OCH_2CH_2OMe)]_2$ and 6-Mes (Ga:6-Mes = 1:1), was in line with the presence of indicated equilibrium. Most probably, the latter was also responsible for the instant reaction of **1** with CD_2Cl_2 resulting in the formation of $[Me_2Ga(\mu\text{-}OCH_2CH_2OMe)]_2$ and $[6\text{-Mes-D}]^+$, which were evidenced by NMR spectroscopy (see the Supplementary Materials). Interestingly, similar reactivity was observed for the reaction between free SIMes and methylene chloride. On the contrary, more acidic chloroform was required in order to react instantly with *N*-heterocyclic carbene of Me_2GaOR(SIMes), while the latter remained essentially stable in CD_2Cl_2 during the NMR experiment [1]. While the presence of the equilibrium presented in Scheme 1 is not surprising in the light of similar equilibrium observed in the case of $Me_2In(OCH(Me)CO_2Me)$(NHC) (NHC = SIMes, IMes) [3], the one observed for **1** represents the first such equilibrium for Me_2GaOR(NHC) complexes, which is in line with the weaker Ga–$C_{6\text{-Mes}}$ bond in comparison with Me_2GaOR(NHC) (NHC = SIMes, IMes). On the contrary, the shift between free 6-Mes (Δ = 244.9 ppm) and coordinated 6-Mes in the case of **1** (197.1 ppm, Δ = −47.8 ppm) was considerably larger in comparison with Me_2MOR(NHC) (NHC = SIMes (Δ = −43.5–(−45.2) ppm), IMes (Δ = −43.1–(−43.6) ppm) [1,2]. Although the latter could indicate the presence of stronger Ga–$C_{6\text{-Mes}}$ bond in solution [25], it rather reflects the stronger donor properties of 6-Mes vs SIMes/IMes in the light of both the structure of **1**, as well as the weaker Ga–$C_{6\text{-Mes}}$ evidenced by the X-ray analysis of $Me_2Ga(OCPh_2Me)$(6-Mes) (**3**) (see below). While the carbene carbon signal in ^{13}C NMR could not be observed for Me_2GaOMe(6-Mes), which was synthesized analogously to **1**, the ^{1}H NMR was in line with the presence of the equilibrium presented in Scheme 1 (see the Supplementary Materials), and therefore, similarly to **1**, indicated weaker Ga–$C_{6\text{-Mes}}$ bond in comparison with Ga–C_{NHC} of Me_2GaOMe(NHC) (NHC = SIMes, IMes).

Despite the adverse effect of steric hindrances of 6-Mes on the strength of Ga–$C_{6\text{-Mes}}$ bond, the stronger donor properties of 6-Mes in comparison with SIMes/IMes, prompted us to investigate its effect on the synthesis and structure of Me_2InOR(NHC) complexes. The main question was,

whether the larger radius of indium, in comparison with gallium, could allow for the formation of a stronger In–$C_{6\text{-Mes}}$ bond and the stabilization of $Me_2InOR(NHC)$, which had been previously shown by us to be unstable and prone to ligand disproportionation [3]. Although the reaction between $[Me_2In(\mu\text{-}OCH_2CH_2OMe)]_2$ and 6-Mes led to the formation of $Me_2In(OCH_2CH_2OMe)$(6-Mes), the latter complex disproportioned readily to Me_3In(6-Mes) and Mitsubishi type complex $In\{Me_2In(\mu\text{-}OCH_2CH_2OMe)\}_3$ (Scheme 2) (see the Supplementary Materials), analogously to $Me_2In(OCH_2CH_2OMe)$(NHC) (NHC = SIMes, IMes) [3]. The formation of both Me_3In(6-Mes) and $In\{Me_2In(\mu\text{-}OCH_2CH_2OMe)\}_3$ was evidenced by NMR spectroscopy, while, in contrast to our previous studies, $In\{Me_2In(\mu\text{-}OCH_2CH_2OMe)\}_3$ could be isolated as a white crystalline solid, similar to the only two other examples of Mitsubishi type indium $In\{Me_2In(\mu\text{-}OR)\}_3$ complexes [27,28]. Unfortunately, we did not succeed in obtaining crystals of $In\{Me_2In(\mu\text{-}OCH_2CH_2OMe)_2\}_3$ suitable for X-ray analysis, and its structure has been confirmed using ^1H and ^{13}C NMR spectroscopy (see the Supplementary Materials).

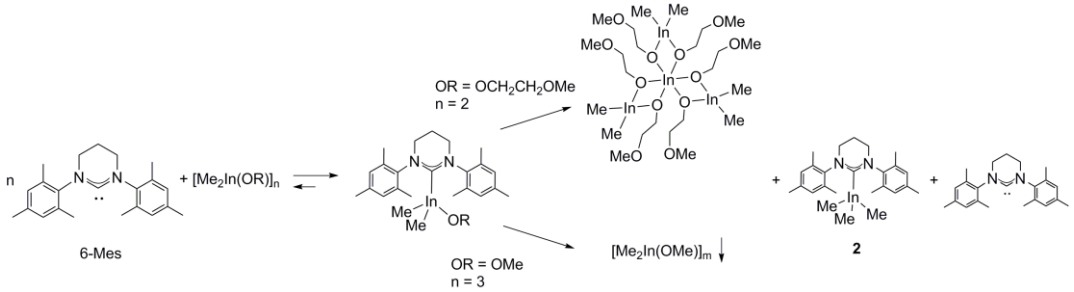

Scheme 2. Synthesis and ligand disproportionation of Me_2InOR(6-Mes).

Although the reaction of 6-Mes with $[Me_2In(\mu\text{-}OMe)]_3$ led to the formation of Me_2InOMe(6-Mes) complex (see the Supplementary Materials), which was more stable in comparison with $Me_2In(OCH_2CH_2OMe)$(6-Mes), it seemed to disproportionate more readily in comparison with Me_2InOMe(NHC) (NHC = SIMes, IMes), and as result could not be isolated in contrast to the latter [3]. While we could not estimate the strength of In-$C_{6\text{-Mes}}$ in the case of Me_2InOR(6-Mes), due to the tendency of the latter to disproportionate , it could be analyzed for the Me_3In(6-Mes) (**2**). The crystals of **2** suitable for X-ray analysis could be obtained either by the decomposition of $Me_2In(OCH_2CH_2OMe)$(6-Mes) or quantitative reaction between 6-Mes and Me_3In. Compound **2** was synthesized and isolated in bulk using only the second method, and was used to confirm the formation of **2** in solution due to the decomposition of $Me_2In(OCH_2CH_2OMe)$(6-Mes). X-ray diffraction analysis of **2** revealed, similarly to Me_3In(NHC) (NHC = SIMes, IMes) monomeric structure, with the coordination sphere adopting a distorted-tetrahedral geometry (Figure 2). The In–$C_{6\text{-Mes}}$ bond (2.367(2) Å, 0.51 valence units (vu) [29]) in **2** turned out to be noticeably longer, and therefore weaker, than In–C_{SIMes} (2.334(6) Å, 0.55 vu [3]; 2.316(8) Å [23]), In–C_{IMes} (2.307(2) Å, 0.60 vu [3]; 2.304(7) Å [23], 2.292(6) Å [21]), In–C_{SIPr} (2.342(2) Å) [23] and In–C_{IPr} (2.309(2) Å) [23] in Me_3In(SIMes), Me_3In(IMes), Me_3In(SIPr) and Me_3In(IPr) adducts, respectively. It showed a more significant effect of steric hindrances of 6-Mes, in comparison with SIMes, IMes, and even SIPr and IPr, on the strength of In–$C_{6\text{-Mes}}$ bond. Interestingly, the latter was in agreement with smaller steric hindrances of SIMes and IMes, and in contrast with larger steric demand of SIPr and IPr, in comparison with 6-Mes, as represented by the buried volume of discussed NHCs [25]. The analysis of the strength of In–$C_{6\text{-Mes}}$ bond of **2** in solution, in comparison with In–C_{NHC} bonds of already characterized Me_3In(NHC) adducts [3,21,23], was in sharp contrast with the solid state result. In solution, the shift between free and coordinated NHCs in ^{13}C NMR, indicated stronger In–$C_{6\text{-Mes}}$ bond (δ = 207.5 ppm, Δ = −37.4 ppm) in comparison with In-C_{SIMes} (Δ = −35.2 ppm) and In–C_{IMes} (Δ = −35.7 ppm) of Me_3In(SIMes) and Me_3In(IMes) respectively. While the relationship between the distance of essentially the same bonds and their strength should be considered a tenet in the case of interpretations of molecular structures [30], the analysis of the strength of a M–C_{NHC} bond using the ^{13}C NMR

spectroscopy could be influenced by other factors affecting the distribution of electron density at carbene carbon. However, it must be noticed that the shift between free and coordinated NHCs in solution, using ^{13}C NMR spectroscopy, reflected stronger donor properties of 6-Mes in comparison with SIMes and IMes. Notably, analogous results concerning the strength of M–C_{NHC} bonds were obtained for alkoxide derivatives $Me_2M(OCPh_2Me)$(6-Mes) (M = Ga, In).

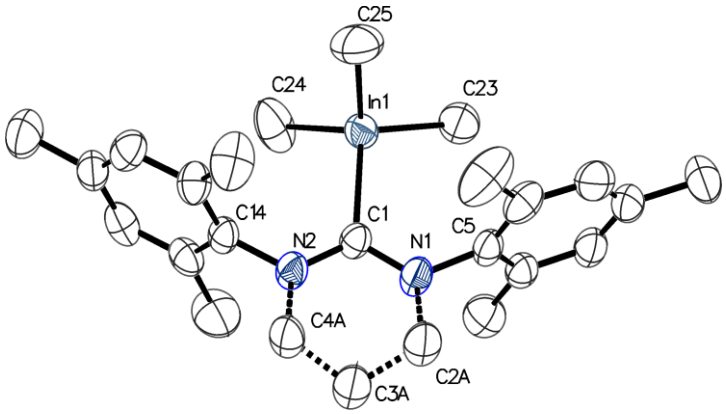

Figure 2. Molecular structure of **2** with thermal ellipsoids at 50% probability level. Selected bond lengths [Å] and angles [°]: In(1)–C(1) 2.367(2), In(1)–C(25) 2.185(3), In(1)–C(24) 2.179(3), In(1)–C(23) 2.198(3), C(23)–In(1)–C(1) 112.04(9), C(24)–In(1)–C(1) 110.26(10), C(25)–In(1)–C(1) 104.99(11), C(24)–In(1)–C(23) 107.31(12), C(24)–In(1)–C(25) 112.31(15), C(25)–In(1)–C(23) 110.00(14), N(1)–C(1)–N(2) 116.75(19), NHC tilt 7.0(1), 5.6(1) (The tilt is quantified by the offset angle of the M–C bond to the C_2 axis of the NHC (defined by C(1) and the centroid of C(2) and C(4)), which is split into pitch and yaw angles [31,32]).

2.2. Reactivity of [$Me_2M(\mu$-$OCPh_2Me)]_2$ (M = Ga, In) towards 6-Mes

While the reaction between $[Me_2Ga(\mu\text{-}OCPh_2Me)]_2$ and 6-Mes (Ga:6-Mes = 1:1, Scheme 3) resulted in the formation of $Me_2Ga(OCPh_2Me)$(6-Mes) (**3**), the prolonged time of 24 h was required to reach c.a. 87% of conversion. Monitoring of the reaction progress using ^1H NMR revealed significantly slower reaction in comparison with the essentially instant reaction of $[Me_2Ga(\mu\text{-}OCPh_2Me)]_2$ with less sterically demanding carbenes (i.e., SIMes, IMes) [3], therefore indicating the strong adverse effects of 6-Mes steric hindrances on its reactivity towards dimeric $[Me_2Ga(\mu\text{-}OCPh_2Me)]_2$ and formation of monomeric $Me_2Ga(OCPh_2Me)$(6-Mes) (**3**) (Scheme 3). The analogous effect was not observed in the case of the reaction of $[Me_2In(\mu\text{-}OCPh_2Me)]_2$ with 6-Mes (In:6-Mes = 1:1, Scheme 3), leading to the formation of the indium complex $Me_2In(OCPh_2Me)$(6-Mes) (**4**), which can be explained by the significantly larger radius of indium in comparison with gallium. Complexes **3** and **4** were isolated in high yields as colorless crystals.

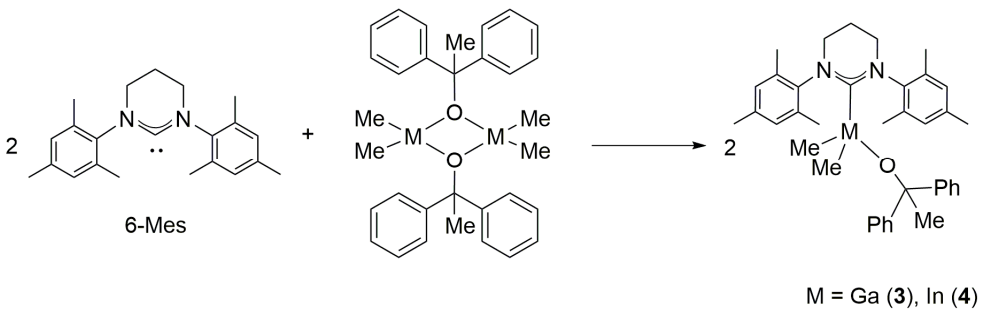

Scheme 3. Synthesis of $Me_2M(OCPh_2Me)$(6-Mes) complexes (M = Ga, In).

For complexes **3** and **4** X-ray diffraction analysis revealed the presence of four-coordinated gallium/indium species with the coordination sphere adopting a distorted-tetrahedral geometry. Interestingly, in contrast to essentially symmetrical gallium complex **3** (Figure 3), due to the orientation of the 6-Mes ligand with respect to In–C_{Me} bonds, the presence of essentially asymmetrical indium complex **4** (Figure 4) was observed. These observations, reflected by O(1)–Ga(1)–C(1)–N(1) (–81.98(15)°) (Figure 3) and O(1)–In(1)–C(1)–N(1) (–139.0(8)°) (Figure 4) torsion angles, were in line with the previously characterized essentially symmetric $Me_2Ga(OCPh_2Me)$(IMes) and asymmetric $Me_2In(OCPh_2Me)$(IMes) complexes [3]. While for **3** and **4** the symmetrical/asymmetrical orientation of NHC in the solid state, with respect to M–C_{Me} (M = Ga, In) bonds, could be tentatively explained by the presence of different weak CH···π interactions, leading to the formation of chains in the solid state (see the Supplementary Materials), the essentially analogous CH···π interactions had been previously observed for $Me_2Me(OCPh_2Me)$(IMes) (M = Ga, In) [3]. Although the symmetrical/asymmetrical orientation of NHC with respect to M–C_{Me} bonds could influence the catalytic properties, including stereoselectivity, of Me_2MOR(NHC), and is of our current interest, the factors controlling the arrangement of NHC in the case of **3** and **4** could not be unequivocally indicated. However, it was the effect of M–$C_{6\text{-Mes}}$ bond on the structure and reactivity of Me_2MeOR(6-Mes), which focused our attention. In the case of complex **3**, the Ga–$C_{6\text{-Mes}}$ bond (2.139(2) Å, 0.57 vu) was significantly weaker in comparison with the Ga–C_{IMes} bond of $Me_2Ga(OCPh_2Me)$IMes (2.096(4) Å, 0.64 vu) [3], although similarly small pitch angles (out of NHC plane tilting) and yaw angles (in plane tilting) were observed for both gallium complexes. Moreover, the longest Ga–$C_{6\text{-Mes}}$ bond of **3**, among other crystallographically characterized Me_2GaOR(NHC) complexes [1–3], should be expected to result from steric hindrances of 6-Mes. Although the In–$C_{6\text{-Mes}}$ bond of **4** (2.329(10) Å, 0.56 vu) was also weaker in comparison with the In–C_{IMes} bond of $Me_2In(OCPh_2Me)$IMes (2.301(8) Å, 0.61 vu), the smaller effect of the steric hindrances of 6-Mes on the In–$C_{6\text{-Mes}}$ bond should be explained by a larger radius of indium in comparison with gallium. Interestingly, the latter resulted in only slightly weaker In–$C_{6\text{-Mes}}$ bond of **4** (2.329(10) Å, 0.56 vu) in comparison with Ga–$C_{6\text{-Mes}}$ bond (2.139(2) Å, 0.57 vu) of **3**.

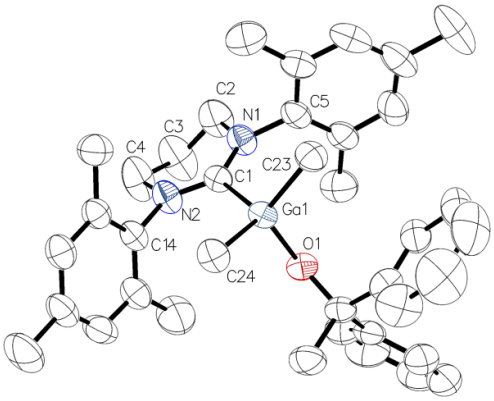

Figure 3. Molecular structure of **3** with thermal ellipsoids at 50% probability level. Selected bond lengths [Å] and angles [°]: Ga(1)–O(1) 1.8849(12), Ga(1)–C(1) 2.1386(19), Ga(1)–C(23) 1.9879(19), Ga(1)–C(24) 1.982(2), O(1)–Ga(1)–C(1) 92.73(6), O(1)–Ga(1)–C(24) 111.74(8), O(1)–Ga(1)–C(23) 116.40(8), C(24)–Ga(1)–C(23) 107.87(9), C(24)–Ga(1)–C(1) 115.30(8), C(23)–Ga(1)–C(1) 112.48(8), N(2)–C(1)–N(1) 116.58(17), O(1)–Ga(1)–C(1)–N(1) −81.98(15), NHC tilt 4.42(9) (The tilt is quantified by the offset angle of the M–C bond to the C_2 axis of the NHC (The tilt is quantified by the offset angle of the M–C bond to the C_2 axis of the NHC (defined by C(1) and the centroid of C(2) and C(4)), which is split into pitch and yaw angles [31,32]).

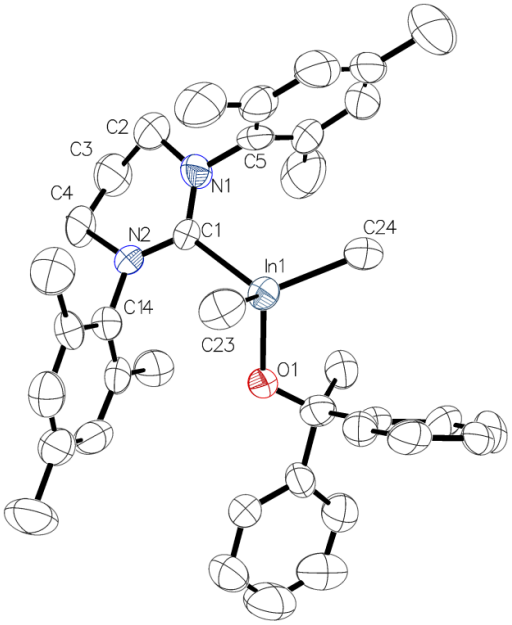

Figure 4. Molecular structure of **4** with thermal ellipsoids at 50% probability level. Selected bond lengths [Å] and angles [°]: In(1)–O(1) 2.081(8), In(1)–C(1) 2.331(10), In(1)–C(23) 2.180(13), In(1)–C(24) 2.154(13), O(1)–In(1)–C(1) 100.9(3), O(1)–In(1)–C(24) 109.0(4), O(1)–In(1)–C(23) 108.3(4), C(24)–In(1)–C(23) 114.4(6), C(24)–In(1)–C(1) 115.3(5), C(23)–In(1)–C(1) 107.9(5), N(1)–C(1)–N(2) 115.6(8). O(1)–In(1)–C(1)–N(1) −139.0(8), NHC tilt 1.0(5)(The tilt is quantified by the offset angle of the M–C bond to the C_2 axis of the NHC (The tilt is quantified by the offset angle of the M–C bond to the C_2 axis of the NHC (defined by C(1) and the centroid of C(2) and C(4)), which is split into pitch and yaw angles [31,32]).

While the major set of signals revealed by the ^{1}H NMR of **3** and **4** was in line with the formation of $Me_2M(OCPh_2Me)$(6-Mes) (M = Ga, In), the presence of minor signal could be ascribed to the $[Me_2Ga(\mu\text{-}OCPh_2Me)]_2$, therefore suggesting the presence of equilibrium, analogously to **1**. However, due to relatively slow reaction rate between $[Me_2M(\mu\text{-}OCPh_2Me)]_2$ and 6-Mes (see above), the presence of minor set of signals could not be unequivocally associated with the equilibrium. The different ratios of $Me_2M(OCPh_2Me)$(6-Mes):$[Me_2Ga(\mu\text{-}OCPh_2Me)]_2$ both in the reaction mixture, as well as in the spectrum of **3** or **4** were not clearly indicative of the presence of such equilibrium. In the ^{13}C NMR of both **3** and **4**, significant shifts of carbene carbon signals between free and coordinated 6-Mes were observed. In the case of gallium complex **3**, the observed shift (Δ = 47.5 ppm) was comparable with $Me_2Ga(OCH_2CH_2OMe)$(6-Mes) (Δ = −47.8 ppm), and slightly smaller than for $Me_2Ga((S)\text{-}OCH(Me)CO_2Me)$(6-Mes) ($\Delta$ = −48.4 ppm) (see below), but was larger in comparison with Me_2GaOR(NHC) (NHC = SIMes, IMes) complexes (Δ_{max} = −45.2 ppm) [2]. Similarly, for **4** the observed shift (Δ = −41.7 ppm) was larger in comparison with Me_2InOR(NHC) complexes (NHC = SIMes, IMes) (Δ_{max} = −38.9 ppm) [3]. However, in the light of X-ray analysis of **3** and **4**, which revealed weaker M–$C_{6\text{-Mes}}$ bonds (M = Ga, In) in comparison with M–C_{NHC} of $Me_2M(OCPh_2Me)$(NHC) (M = Ga, In; NHC = SIMes, IMes), the shift of carbene carbon observed in ^{13}C NMR was indicative, similarly to **1** and **2**, of the stronger donor properties of 6-Mes in comparison with SIMes or IMes, rather than stronger M–$C_{6\text{-Mes}}$ bonds in comparison with M–C_{NHC} (NHC = SIMes, IMes). While the detailed discussion on the factors affecting the carbene carbon shift in ^{13}C NMR, and therefore the analysis of the strength of the M–C_{NHC} bond using the ^{13}C NMR spectroscopy, cannot be done at the current stage, our present research in this area focuses on the effect of the character of the M–C_{NHC} bond, rather than only its strength, on the synthesis, structure and reactivity of group 13 metal Me_2MOR(NHC) complexes.

2.3. Reactivity of $[Me_2M(\mu\text{-}OC_6H_4OMe)]_2$ (M = Ga, In) towards 6-Mes

Although the investigation of the synthesis and structure of $Me_2M(OC_6H_4OMe)$(6-Mes) (M = Ga (**5**), In (**6**)) (Scheme 4) was important prior to the studies on their catalytic activity in the ring-opening polymerization (ROP) of *rac*-lactide (*rac*-LA) (see below), they were also interesting with regard to our studies on $Me_2Ga(O,C_{NHC})$ complexes possessing chelate alkoxide and aryloxide ligands with NHC functionality [33]. The latter showed that aryloxide (O_{Ar},C_{NHC}) ligands, in comparison with alkoxide chelate (O,C_{NHC}) ligands, resulted in stronger Ga–C_{NHC} bond, which could be crucial for the synthesis and structure of **5** and **6** in comparison with their alkoxide analogues Me_2MOR(6-Mes) (M = Ga, In). The reactions of 6-Mes with $[Me_2M(\mu\text{-}OC_6H_4OMe)]_2$ (M:6-Mes = 1:1, M = Ga, In) led to the instant formation of **5** and **6**, which were isolated in high yields as white crystalline solids. However, the crystals suitable for X-ray analysis could not be isolated. Therefore, the structure of **5** and **6** was determined in solution using NMR spectroscopy.

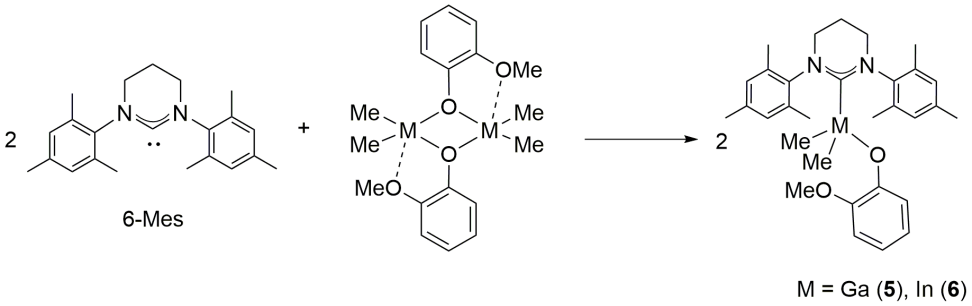

Scheme 4. Synthesis of $Me_2M(OC_6H_4OMe)$(6-Mes) complexes (M = Ga, In).

Importantly, ^{1}H NMR spectra of **5** and **6**, which were essentially identical to the corresponding reaction mixtures of $[Me_2M(\mu\text{-}OC_6H_4OMe)]_2$ (M = Ga, In) and 2 equivalents of 6-Mes, revealed only one set of signals of $Me_2M(OC_6H_4OMe)$(6-Mes). The lack of any signals corresponding to $[Me_2M(\mu\text{-}OC_6H_4OMe)]_2$, indicating the presence of the equilibrium analogues to that of **1**, could be associated in this case both with the significantly weaker M_2O_2 central bridges of dialkylgallium and dialkylindium aryloxides, in comparison with respective alkoxide derivatives, and stronger M–$C_{6\text{-Mes}}$ bonds in the case of aryloxide complexes **5** and **6**. These observations were in line with the shift between free and coordinated carbene carbon signal in ^{13}C NMR for **5** (196.1 ppm, Δ = –48.8 pm), which was only slightly different from **1** (Δ = −47.8 ppm) and **3** (Δ = −47.5 ppm), and considerably larger in comparison with Me_2GaOR(NHC) (NHC = SIMes, IMes; Δ_{max} = −44.8 ppm) complexes, as well as $Me_2Ga(O_{Ar})$(SIMes) (Δ = −45.2 ppm) [34]. In the case of **6**, the carbene carbon of 6-Mes in ^{13}C NMR (204.3 ppm, −40.6 ppm) was only slightly shifted to the higher field in comparison with Me_2InOR(NHC) (NHC = SIMes, IMes; Δ_{max} = −38.9 ppm), and even slightly shifted to the lower field in contrast to **4** (Δ = −41.7 ppm). However, the observed carbene carbon shifts could not be directly related to the stronger M–$C_{6\text{-Mes}}$ bond in **5** and **6**, in comparison with alkoxide-$Me_2M(OR)$(NHC), and aryloxide-$Me_2Ga(O_{Ar})$(NHC) complexes [1–3], in the light of the structure of **1**–**4**.

2.4. Reactivity of $[Me_2M(\mu\text{-}(S)\text{-}OCH(Me)CO_2Me)]_2$ (M = Ga, In) towards 6-Mes

The synthesis and structure of $Me_2M((S)\text{-}OCH(Me)CO_2Me)$(6-Mes) ($Me_2Ga((S)$-*melac*)(6-Mes)) (M = Ga, In), in which the methyl lactate (*melac*) ligand mimics a growing polylactide (PLA) chain [1,2,35–37], were investigated prior to the studies on the activity of Me_2MOR(6-Mes) in the ROP of *rac*-LA (see below). Although both gallium and indium complexes could not be isolated in this case, among others due to the reactivity of 6-Mes with (*S*)-*melac* ligand, they were indicative of the reactivity of sterically hindered NHCs towards methyl lactate ligands, as well as indicative of the structure and reactivity of $Me_2M(O(PLA))$(NHC) propagating species in the ROP of *rac*-LA. The reaction of $[Me_2Ga(\mu\text{-}(S)\text{-}melac)]_2$ with 6-Mes (Ga:6-Mes = 1:1) resulted in the formation of $Me_2Ga((S)$-*melac*)(6-Mes),

which was evidenced both by ^{1}H NMR and ^{13}C NMR spectroscopy (see the Supplementary Materials). The presence of two singlets at −1.10 and −1.14 ppm, considerably shifted to higher field in comparison with [Me_2Ga(μ-(*S*)-*melac*)]$_2$, could be unequivocally ascribed to Ga–Me protons of Me_2Ga((*S*)-*melac*)(6-Mes) on the basis of our earlier studies on Me_2Ga((*S*)-*melac*)(NHC) (NHC = SIMes, IMes) [1,2]. Additionally, the considerable shift of carbene carbon signal in the ^{13}C NMR spectra (196.5 ppm, Δ = −48.4 ppm) was in line with the formation of Ga–$C_{6\text{-Mes}}$ bond. However, the presence of additional signals in the ^{1}H NMR spectra, including broad signal at −0.03 ppm indicated the presence of other alkylgallium species, most probably without 6-Mes coordinated to gallium. The presence of the latter signal could be associated, similarly to the synthesis of **3**, with Me_2Ga protons of unreacted [Me_2Ga(μ-(*S*)-*melac*)]$_2$. However, further monitoring of the reaction in time, which revealed an exclusive presence of a signal at −0.02 ppm after 4 days, suggested that initially observed broad signal at −0.03 ppm could rather result from the transformation of (Me_2Ga((*S*)-*melac*)(6-Mes)) to new alkylgallium species. While the instability of (Me_2Ga((*S*)-*melac*)(6-Mes)) was in contrast with the strong Ga–$C_{6\text{-Mes}}$ bond, the reactivity of 6-Mes towards methyl lactate ligand could be expected, based on the reactivity of SIPr towards (*S*)-*melac* ligand of [Me_2Ga(μ-(*S*)-*melac*)]$_2$, which led to the formation of among others [Me_2Ga(OCH(Me)CO_2)][SIPr-H] [2]. However, the possible equilibrium between Me_2M(O-(*S*)-CH(Me)CO_2Me)(6-Mes) and [Me_2Ga(*μ-(S)-melac*)]$_2$/6-Mes mixture, as revealed by the structure of **1**, could result in the complete reaction of 6-Mes with (*S*)-*melac*, leading to the formation of a complex mixture of products, as shown in Scheme 5. Although no alkylgallium species could be isolated from the reaction mixture of [Me_2Ga(*μ-(S)-melac*)]$_2$ with 6-Mes (Ga:6-Mes = 1:1) the obtained results were in line with the reactivity of 6-Mes towards *(S)-melac*) of Me_2M(*(S)-melac*)(6-Mes) presented in Scheme 5, which was suggested on the basis of the reaction of [Me_2Ga(*μ-(S)-melac*)]$_2$ with SIPr (Ga:SIPr = 1:1) [2], as well as the reactivity of [MeIn(*μ-(S)-melac*)]$_2$ with 6-Mes (In:6-Mes = 1:1). Contrary to the reactivity of [MeGa(*μ-(S)-melac*)]$_2$ with 6-Mes, the formation of monomeric Me_2In*((S)-melac*)(6-Mes) was not even indicated by ^{1}H NMR in the analogous reaction between [MeIn(*μ-(S)-melac*)]$_2$ and 6-Mes (In:6-Mes = 1:1) (see the Supplementary Materials). Moreover, in contrast to the formation of unstable Me_2In*((S)-melac*)(NHC) (NHC = SIMes, IMes), which showed the tendency for the ligand disproportionation and the formation of Me_3In(NHC) and alkylindium alkoxides [3], the reactivity of 6-Mes towards *(S)-melac*) was confirmed by the isolation of (6-Mes)=CH_2, which was evidenced by X-ray analysis (Figure 5). Interestingly, the formation of the latter confirmed the possibility of the abstraction of Me^+ from *(S)-melac* ligand with NHC, which was only suggested in the case of our previous studies by the formation of [Me_2Ga(OCH(Me)CO_2)]$^-$. Moreover, the isolation of (6-Mes)=CH_2 strongly indicated the conversion of [(6-Mes)-Me]$^+$ to (6-Mes)=CH_2 with the evolution of H^+. The latter could be responsible for the formation of [(6-Mes)-H]$^+$, leading to the complex mixture of products. Moreover, it could also explain the formation of SIPr-H$^+$ in our previous reaction of [Me_2Ga(*μ-(S)-melac*)]$_2$ with SIPr (Ga:SIPr = 1:1) (Scheme 5), instead of the possible abstraction of H^+ directly from (*S*)-*melac* ligand, which was tentatively suggested in the latter case [2].

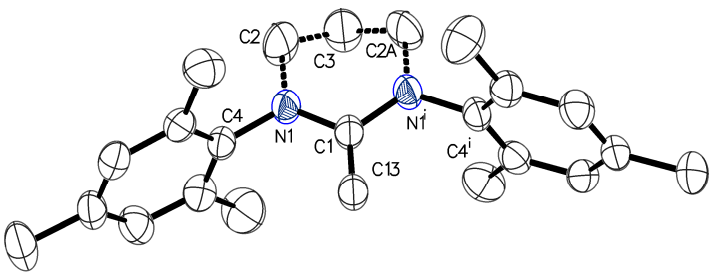

Figure 5. Molecular structure of (6-Mes)=CH_2 with thermal ellipsoids at 50% probability level. Selected bond lengths [Å] and angles [°]: C(1)–N(1) 1.3875(18), C(1)–C(13) 1.336(3), C(1)–N(1)–C(13) 122.43(10).

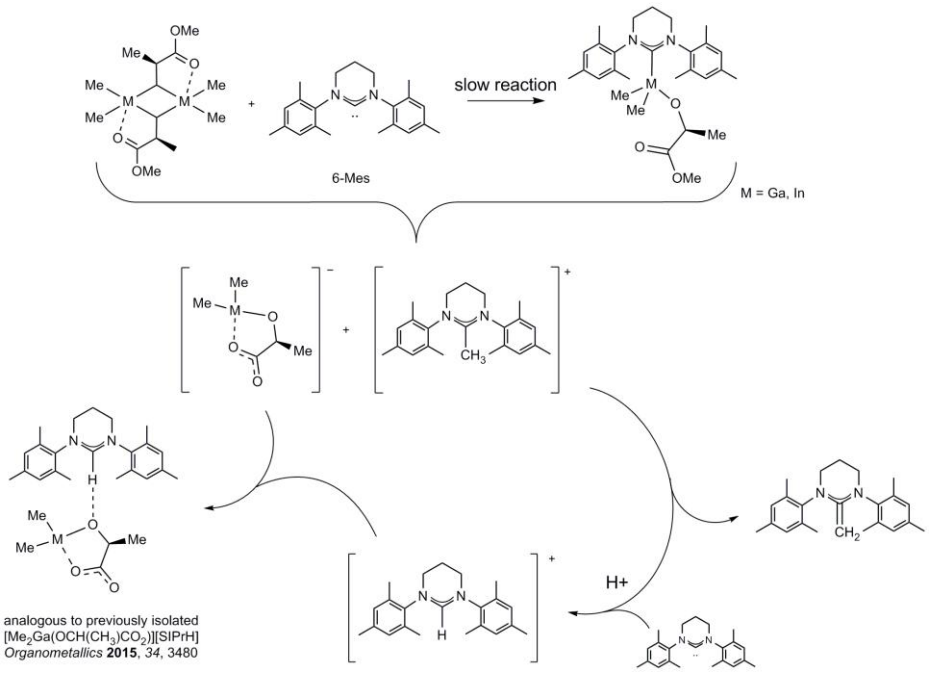

Scheme 5. Reactivity of $[Me_2M((S)\text{-}OCH(Me)CO_2Me)]_2$ towards 6-Mes.

*2.5. Activity of $Me_2Ga(OCPh_2Me)$(6-Mes) (**3** and **4**), $Me_2M(OC_6H_4OMe)$(6-Mes) (**5** and **6**) (M = Ga, In) and $Me_2Ga(OCH_2CH_2OMe)$(6-Mes) (**1**) in the ROP of rac-Lactide*

In order to investigate the effect of 6-Mes on the catalytic properties of $Me_2MOR(NHC)$, we examined the activity of **1**, **3**, **4**, **5** and **6** complexes in the ring-opening polymerization (ROP) of *rac*-LA. With regard to the latter, we focused on the effect of M–$C_{6\text{-Mes}}$ bond on the catalytic properties of selected complexes. While the M–$C_{6\text{-Mes}}$ bond affects the structure of all selected complexes, it should be expected to influence their reactivity, as well the structure and reactivity of $Me_2MO(PLA)$(6-Mes), where O(PLA) represents growing polylactide chain, and therefore the microstructure of resulting polylactide (PLA). While our previous results showed that both gallium and indium $Me_2MOR(NHC)$ complexes were highly active already at −20 °C [1–3], in order to compare our results with the latter, we investigated the ROP of *rac*-LA with **1**, **3**, **4**, **5** and **6** at identical conditions. Gallium complexes: alkoxide derivative $Me_2M(OCPh_2Me)$(6-Mes) (**3**) and aryloxide derivative $Me_2Ga(OC_6H_4OMe)$(6-Mes) (**5**), were inactive in the polymerization of *rac*-LA at −20 °C. While in the case of complexes **3** and **5** the bulky alkoxide or aryloxide group did not allow for the insertion of *rac*-LA into Ga–O bond, most importantly, the strong Ga–$C_{6\text{-Mes}}$ bond precluded, the initiation of *rac*-LA polymerization by *N*-heterocyclic carbene, similarily to $Me_2Ga(OCPh_2Me)(NHC)$ (NHC = SIMes, IMes) [3]. Contrary to the latter, a much weaker In–C_{NHC} bond in $Me_2In(OCPh_2Me)(NHC)$ (NHC = SIMes, IMes) resulted in the initiation of *rac*-LA by *N*-heterocyclic carbenes [3], and similar reactivity was observed in the case of $Me_2In(OCPh_2Me)$(6-Mes) (**4**) and $Me_2In(OC_6H_4OMe)$(6-Mes) (**6**), which led to the formation of cyclic PLA (see the Supplementary Materials). However, the observed reactivity of 6-Mes of indium complexes **4** and **6** towards lactide, as well as the lack of activity of gallium derivatives **3** and **5**, may also indicate the considerable effect of a character of the M–C_{NHC} bond on the reactivity of investigated complexes. As we were unable to isolate any stable alkoxide Me_2InOR(6-Mes) complex, we focused on the activity of **1** in the ROP of *rac*-LA. Due to the reactivity of **1** towards CH_2Cl_2, which led to the almost quantitative and instant formation of $[Me_2Ga(\mu\text{-}OCH_2CH_2OMe)]_2$ [9,35], no activity of **1** in the ROP of *rac*-LA in CH_2Cl_2, at −20 °C was observed. On the other hand, the polymerization of *rac*-LA with **1** (25:1) in toluene led to essentially full conversion after 12 h (−20 °C) or 10 min (room temperature). For the PLA obtained at both temperatures the MALDI-TOF analysis revealed the presence of an end group of 76 Da, which was in agreement with the insertion of *rac*-LA into Ga–OCH_2CH_2OMe

bond (see the Supplementary Materials). Additionally, for PLA obtained at both −20 °C and r.t. the extensive intermolecular transesterification was evidenced, while minor distributions referring to cyclic PLA could be assigned to the presence of an intermolecular transesterification or additional initiation of *rac*-LA ROP by 6-Mes. Although the initiation of the lactide polymerization by 6-Mes of **1**, especially at −20 °C, was unlikely in the light of the lack of activity of **3** and **5**, it could be assumed for Me_2GaO(PLA)(6-Mes) propagating species. However, as we were not able to synthesize Me_2Ga(*(S)-melac*)(6-Mes) (see above), which mimics propagating species Me_2GaO(PLA)(6-Mes), we synthesized the latter in the reaction between **1** and 10 equiv of *rac*-LA both at −20 °C and r.t.. Although the ^{1}H NMR spectra after 36 h, both at −20 °C and r.t. were essentially the same, as the spectrum registered after mixing of **1** and 10 equiv of *rac*-LA at room temperature, they were inconclusive for the presence of Me_2GaO(PLA)(6-Mes) with 6-Mes coordinated to gallium. In this case, the presence of complex Ga–Me signals in ^{1}H NMR in the range between −0.31 and 0.02 was in contrast to Me_2Ga((*S*)-*melac*)(SIMes) (−0.80, −0.82 ppm) or $Me_2Ga(OCH(Me)C(O))_2O(CH_2)_2OMe$(IMes) (−0.79, −0.87 ppm) [2], and could not strongly support the presence of Me_2GaO(PLA)(6-Mes). Moreover, the lack of signal corresponding to coordinated/uncoordinated carbene carbon in ^{13}C NMR was also inconclusive for the formation of the latter. Therefore, we could not unequivocally conclude whether the initiation of the ROP of *rac*-LA by 6-Mes was possible, or the presence of discussed transesterification reactions simply resulted from the catalytic properties of Me_2GaO(PLA)(6-Mes) propagating species. However, irrespective of the origin, the presence of transesterification in the case of the ROP of *rac*-LA with **1** at –20 °C, which is in contrast with the essentially no transesterification observed for the ROP of *rac*-LA with Me_2GaOR(NHC) (NHC = SIMes, IMes) [1,2], led to a considerable decrease of isoselectivity (P_m (probability of *meso* linkages in PLA) = 0.66–0.69 at −20 °C, P_m = 0.63–0.66 at r.t.) in comparison with the ROP of *rac*-LA with Me_2GaOR(NHC) (P_m = 0.76–0.78 at −20 °C, P_m = 0.65–0.68 at r.t.). Importantly, the ROP of *rac*-LA with **1** showed the considerable effect of the structure of NHC on the catalytic properties of Me_2GaOR(NHC), which should be of importance and is of our current interest as Me_2GaOR(NHC) are still rare examples of highly active metal alkoxides for the isoselective ROP of *rac*-LA [5–13].

3. Materials and Methods

3.1. General Procedures

All operations were carried out under dry argon using standard Schlenk techniques. Solvents and reagents were purified and dried prior to use. Solvents were purified using MBRAUN Solvent Purification Systems (MB-SPS-800) (MBRAUN, Garching, Germany) and stored over molecular sieves. *rac*-Lactide was purchased from Aldrich (Poland) and further purified by crystallization from anhydrous toluene and then sublimated. (*S*)-Methyl lactate, 2-methoxyethanol, and methanol were purchased from Aldrich, dried over molecular sieves, and distilled under argon. 1,1-diphenylethanol was purchased from Aldrich and used as received. Me_3In and Me_3Ga were purchased from STREM Chemicals, Inc. (Bischheim, France) and used as received. 6-Mes was synthesized according to the literature [38]. Indium and gallium complexes: $[Me_2M(\mu\text{-}OCH_2CH_2OMe)]_2$, $[Me_2M(\mu\text{-}OMe)]_3$, $[Me_2M(\mu\text{-}OCH(CH_3)COOMe)]_2$, $(Me_2M(\mu\text{-}OCPh_2Me)]_2$, $Me_2M(OC_6H_4OMe)]_2$ were synthesized as described by us previously [1–3]. ^{1}H and ^{13}C NMR spectra were recorded on an Agilent 400-MR DD2 400 MHz spectrometer (Agilent, Palo Alto, CA, USA) with shifts given in ppm according to the deuterated solvent shift. MALDI-TOF spectra were recorded on a Bruker Model ultrafleXtreme instrument (Bruker Daltonics, Bremen, Germany). Elemental analysis was performed on a Vario EL III instrument (ELEMENTAR Analysensysteme, Hanau, Germany).

3.2. Synthesis of Indium and Gallium Complexes

Synthesis of **1**. To a solution of $[Me_2Ga(\mu\text{-}OCH_2CH_2OMe)]_2$ (76.4 mg, 0.44 mmol) in toluene (2 mL) was added 2 mL of a toluene solution of 6-Mes (140.0 mg, 0.44 mmol) at room temperature, and the resulting solution was stirred for 2 h. Then toluene was removed under vacuum to give a

faint-yellow oil, which turned to an off-white solid after 45 min of drying. The solid was subsequently crystallized from toluene (0.3 mL), Et_2O (4 mL) and hexane (3 mL) at −40 °C to give off-white crystals, which were dried under vacuum (**1**, 158 mg, 73%). Anal. Calcd. for $C_{27}H_{41}GaN_2O_2$: C, 65.47; H, 8.34; N, 5.66. Found: C, 65.32; H, 8.34; N, 5.60. ^{1}H NMR (toluene-d_8, 400 MHz): −1.08 (s, 6H, $GaCH_3$), 1.49 (q, 2H, ^3J (H,H) = 5.9 Hz, $CH_2CH_2CH_2$), 2.11 (s, 6H, CH_3), 2.29 (s, 12H, CH_3), 2.60 (t, 4H, ^3J (H,H) = 5.9 Hz, $CH_2CH_2CH_2$), 3.27 (s, 3H, OCH_3), 3.45 (t, 2H, ^3J (H,H) = 6.5 Hz, CH_2CH_2), 3.69 (t, 2H, ^3J (H,H) = 6.5 Hz, CH_2CH_2), 6.75 (s, 4H, CH_{Ar}). ^{13}C{1H} NMR (toluene-d_8, 100 MHz): −5.6 ($GaMe_2$), 18.2, 20.9, 21.0, 42.0, 47.2, 58.5, 64.0, 77.8, 129.3, 129.8, 135.0, 135.6, 137.7, 141.8, 197.1 (carbene).

Synthesis of **2**. A stirred solution of Me_3In (116 mg, 0.73 mmol) in toluene (5 mL) was cooled to −20 °C, and a toluene solution (2 mL) of 6-Mes (232 mg, 0.73 mmol) was added dropwise. After addition the reaction mixture was warmed to room temperature and stirred for 2 h. Solvent and volatile residues were then removed under vacuum to give a white solid. The solid was subsequently recrystallized from a toluene/hexane solution (2/6 mL) at −20 °C to give white crystals, which were washed twice with 3 mL of hexane and dried under vacuum to give Me_3In(6-Mes) (nr; 311 mg, 92%). Anal. Calcd. for $C_{25}H_{37}InN_2$: C, 62.50; H, 7.76; N, 5.83. Found: C, 62.36; H, 7.88; N, 5.76. ^{1}H NMR (toluene-d_8, 400 MHz): −0.88 (s, 9H, $InCH_3$), 1.50 (m, 2H, CH_2), 2.11 (s, 6H, CH_3), 2.19 (s, 12H, CH_3), 2.58 (m, 4H, CH_2CH_2), 6.77 (s, 4H, CH_{Ar}). ^{13}C{1H} NMR (toluene-d_8, 100 MHz): −8.0 ($InMe_3$), 18.1, 20.9, 46.3, 130.1, 135.1, 137.4, 137.7, 142.1, 207.5 (carbene).

Synthesis of **3** *and* **4**. To a solution of $[Me_2In(\mu\text{-}OCPh_2Me)]_2$ (110 mg, 0.32 mmol) or $[Me_2Ga(\mu\text{-}OCPh_2Me)]_2$ (96 mg, 0.32 mmol) in toluene (6 mL) was added 2 mL of a toluene solution of 6-Mes (103 mg, 0.32 mmol) at room temperature, and the resulting solution was stirred for 24 h. Then, toluene was removed under vacuum to give a light yellow solid. The solid was subsequently crystallized from toluene (2 mL) after addition of hexane (6 mL) at −20 °C to give white crystals, which were dried under vacuum (nr In, 187 mg, 88%; nr Ga, 158 mg, 80%). Data for **4** are as follows. Anal. Calcd. for $C_{38}H_{47}InN_2O$: C, 68.88; H, 7.15; N, 4.23. Found: C, 66.92; H, 7.25; N, 4.17. ^{1}H NMR (toluene-d_8, 400 MHz): −1.30 (s, 6H, $InCH_3$), 1.42 (q, 2H, ^3J (H,H) = 5.9 Hz, $CH_2CH_2CH_2$), 1.78 (s, 3H, CCH_3), 2.14 (s, 6H, CH_3), 2.26 (s, 12H, CH_3), 2.54 (t, 4H, ^3J (H,H) = 5.9 Hz, $CH_2CH_2CH_2$), 6.77 (br s, 4H, CH_{Ar}), 7.03–7.07 (m, 2H, CH_{Ar}), 7.16–7.21 (m, 4H, CH_{Ar}), 7.51 (m, 4H, CH_{Ar}). ^{13}C{1H} NMR (toluene-d_8, 100 MHz): −5.0 ($InMe_2$), 14.3, 18.4, 21.0, 23.1, 32.0, 33.7, 46.4, 77.6, 124.9, 126.9, 127.2, 127.6, 128.4, 129.2, 130.2, 135.6, 138.0, 141.9, 155.7, 203.2 (carbene). Data for **3** are as follows. Anal. Calcd. for $C_{38}H_{47}GaN_2O{\cdot}C_6H_8$(toluene): C, 76.16; H, 7.81; N, 3.95. Found: C, 76.30; H, 8.14; N, 3.80. ^{1}H NMR (toluene-d_8, 400 MHz): −1.36 (s, 6H, $GaCH_3$), 1.45 (q, 2H, ^3J (H,H) = 5.9 Hz, $CH_2CH_2CH_2$), 1.78 (s, 3H, CCH_3), 2.14 (s, 6H, CH_3), 2.25 (s, 12H, CH_3), 2.58 (t, 4H, ^3J (H,H) = 5.9 Hz, $CH_2CH_2CH_2$), 6.74 (s, 4H, CH_{Ar}), 7.04 (m, 2H, CH_{Ar}), 7.17 (m, 4H, CH_{Ar}), 7.46 (m, 4H, CH_{Ar}); ^{13}C{1H} NMR (toluene-d_8, 100 MHz): −1.2 ($GaMe_2$), 17.3, 18.5, 20.9, 21.0, 21.3, 32.6, 47.5, 77.7, 125.0, 125.6, 127.1, 127.8, 128.4, 129.2, 129.9, 135.5, 137.7, 142.0, 154.8, 156.3, 197.4 (carbene).

Synthesis of **5** *and* **6**. To a solution of $[Me_2In(\mu\text{-}OC_6H_4OMe)]_2$ (143 mg, 0.53 mmol) or $[Me_2Ga(\mu\text{-}OC_6H_4OMe)]_2$ (118 mg, 0.53 mmol) in toluene (6 mL) was added 2 mL of a toluene solution of 6-Mes (171 mg, 0.53 mmol) at room temperature, and the resulting solution was stirred for 2 h. Then toluene was removed under vacuum to give a pale white solid. The solid was subsequently crystallized from toluene (1.5 mL) after addition of hexane (5 mL) at −20 °C to give white crystals, which were dried under vacuum (nr In, 283 mg, 90%; nr Ga, 249 mg, 86%). Data for **6** are as follows. Anal. Calcd. for $C_{31}H_{41}InN_2O_2$: C, 63.27; H, 7.02; N, 4.76. Found: C, 63.09; H, 7.20; N, 4.80. ^{1}H NMR (toluene-*d*8, 400 MHz): −1.00 (s, $InCH_3$), 1.56 (q, 2H, ^3J (H,H) = 5.8 Hz, $CH_2CH_2CH_2$), 2.07 (s, 6H, CH_3), 2.31 (s, 12H, CH_3), 2.63 (t, 4H, ^3J (H,H) = 5.8 Hz, $CH_2CH_2CH_2$), 3.29 (s, 3H, OCH_3), 6.49 (m, 2H, CH_{Ar}), 6.67 (br s, 4H, CH_{Ar}), 6.86 (m, 1H, CH_{Ar}), 6.96 (m, 1H, CH_{Ar}); ^{13}C{1H} NMR (toluene-d_8, 100 MHz): −6.7 ($InMe_2$), 18.0, 20.9, 46.5, 54.1, 110.9, 112.7, 118.9, 121.8, 130.2, 135.6, 137.9, 141.8, 150.8, 157.3, 204.3 (carbene). Data for **5** are as follows. Anal. Calcd. for $C_{31}H_{41}GaN_2O_2$: C, 68.52; H, 7.61; N, 5.16. Found: C, 68.22; H, 7.56; N, 5.16. ^{1}H NMR (toluene-d_8, 400 MHz): −1.00 (s, $GaCH_3$), 1.55 (q, 2H, ^{3}J (H,H) = 5.9 Hz, $CH_2CH_2CH_2$), 2.06 (s, 6H, CH_3), 2.29 (s, 12H, CH_3), 2.65 (t, 4H, ^3J (H,H) = 5.9 Hz, $CH_2CH_2CH_2$), 3.55 (s, 3H, OCH_3), 6.54 (m, 1H, CH_{Ar}), 6.62 (m, 1H, CH_{Ar}), 6.67 (br s, 4H, CH_{Ar}), 6.70

(m, 1H, CH_{Ar}), 6.80 (m, 1H, CH_{Ar}); $^{13}C\{1H\}$ NMR (toluene-d_8, 100 MHz): −3.9 ($GaMe_2$), 18.1, 20.9, 47.4, 55.7, 113.3, 114.4, 119.8, 121.7, 129.9, 135.6, 137.8, 141.5, 152.1, 155.9, 196.1 (carbene).

*3.3. General Procedure for the ROP of rac-LA with **1** and **3**–**6***

To a *rac*-LA (334.8 mg, 2.32 mmol, 25 eq) suspension in toluene (10 mL) cooled to −20 °C was added a toluene solution (1 mL) of the catalyst (0.09 mmol, 1 eq), and the reaction was stirred overnight at −20 °C until the *rac*-LA fully dissolved. In the case of polymerization at room temperature, *rac*-LA dissolved fully after 10 min. Each polymerization was quenched by the addition of a HCl solution (5%, 50 mL). The organic phase was separated, washed twice with water (50 mL), dried over anhydrous $MgSO_4$ and dried under vacuum to give PLA as a white solid. ^1H NMR ($CDCl_3$, 400 MHz): (a) PLA signals, 1.46–1.55 (m, 3H, $CHCH_3$), 5.10–5.23 (m, 1H, $CHCH_3$); (b) end groups for PLA obtained with **1** 3.36 (s, 3H, OCH_3), 3.57 (s, 2H, CH_2), 4.26 (s, 2H, CH_2). PLA (~0.2 g) was also precipitated from methylene chloride solution (0.5 mL) with 20 mL of MeOH, filtered off, and dried under vacuum to yield PLA with approximately 70% yield. The precipitated PLA was further analyzed by ^1H NMR, homodec NMR and ^{13}C NMR (see Supplementary Materials).

3.4. X-Ray Structure Determination

Single crystals of **2**, **3**, **4** and (6-Mes)=CH_2 were grown from toluene/hexane solutions. Suitable single crystals were selected under a polarizing microscope and glued to a glass capillary. The diffraction data were collected on an Oxford Diffraction Gemini A ultra diffractometer at room temperature. Data collection and reduction were performed using the CrysAlis^{PRO} software developed by Rigaku Oxford Diffraction [39]. The structures were solved with the ShelXT structure solution program using Intrinsic Phasing and refined with the ShelXL refinement package using Least Squares minimization [40]. These programs were invoked from within Olex2 suite which was also used for the production of Figures 2–5 [41].

Crystal Data for **2**, $C_{25}H_{37}InN_2$ (M = 480.38 g/mol): monoclinic, space group $P2_1/n$ (no. 14), a = 9.5680(3) Å, b = 16.9878(4) Å, c = 16.0384(5) Å, β = 106.868(3)°, V = 2494.73(13) Å^3, Z = 4, T = 293(2) K, μ(Mo$K\alpha$) = 0.959 mm^{-1}, D_{calc} = 1.279 g/cm^3, 22528 reflections measured (6.5° ≤ 2Θ ≤ 52.0°), 4884 unique (R_{int} = 0.0219, R_{sigma} = 0.0162) which were used in all calculations. The final R_1 was 0.0245 ($I > 2\sigma(I)$) and wR_2 was 0.0646 (all data).

Crystal Data for **3**, $C_{38}H_{47}GaN_2O$ (M = 617.49 g/mol): monoclinic, space group $P2_1/c$ (no. 14), a = 11.5312(3) Å, b = 18.7807(5) Å, c = 19.0639(5) Å, β = 100.916(3)°, V = 4053.87(19) Å^3, Z = 4, T = 293(2) K, μ(Mo$K\alpha$) = 0.704 mm^{-1}, D_{calc} = 1.012 g/cm^3, 65065 reflections measured (6.7° ≤ 2Θ ≤ 53.0°), 8392 unique (R_{int} = 0.0504, R_{sigma} = 0.0305) which were used in all calculations. The final R_1 was 0.0373 ($I > 2\sigma(I)$) and wR_2 was 0.0947 (all data).

Crystal Data for **4**, $C_{38}H_{47}InN_2O$ (M =662.59 g/mol): tetragonal, space group $I4_1cd$ (no. 110), a = 28.4159(12) Å, c = 19.2051(10) Å, V = 15507.4(15) Å^3, Z = 16, T = 293(2) K, μ(Mo$K\alpha$) = 0.636 mm^{-1}, D_{calc} = 1.135 g/cm^3, 21599 reflections measured (7.1° ≤ 2Θ ≤ 50.0°), 6490 unique (R_{int} = 0.0763, R_{sigma} = 0.0914) which were used in all calculations. The final R_1 was 0.0505 ($I > 2\sigma(I)$) and wR_2 was 0.1532 (all data).

Crystal Data for (6-Mes)=CH_2, $C_{23}H_{30}N_2$ (M =334.49 g/mol): orthorhombic, space group $Pbcn$ (no. 60), a = 15.7258(15) Å, b = 7.9668(8) Å, c = 16.0813(14) Å, V = 2014.7(3) Å^3, Z = 4, T = 293(2) K, μ(Mo$K\alpha$) = 0.064 mm^{-1}, D_{calc} = 1.103 g/cm^3, 7777 reflections measured (7.2° ≤ 2Θ ≤ 53.0°), 2080 unique (R_{int} = 0.0267, R_{sigma} = 0.0224) which were used in all calculations. The final R_1 was 0.0552 ($I > 2\sigma(I)$) and wR_2 was 0.1570 (all data).

4. Conclusions

In summary, we have investigated the influence of steric and electronic properties of 1,3-bis(2,4,6-trimethylphenyl)-3,4,5,6-tetrahydropyrimidin-1-ylidene (6-Mes) on the synthesis, structure and reactivity of Me_2MOR(NHC). Particularly, we have focused on the M–$C_{6\text{-Mes}}$ bond in Me_2MOR(6-Mes), how it is influenced by the structure of 6-Mes in comparison with other NHCs,

and how it can influence the structure of $Me_2MOR(6\text{-Mes})$ as well as their catalytic activity in the ring-opening polymerization (ROP) of racemic lactide (*rac*-LA). The considerable effect of steric hindrances of 6-Mes was reflected both by significantly longer, and therefore weaker M–$C_{6\text{-Mes}}$ in the solid state in comparison to M–C_{SIMes} and M–C_{IMes}, which was revealed by X-ray analysis and the presence of equilibrium between $Me_2MOR(NHC)$ and $[Me_2M(\mu\text{-OR})]_2$/NHC in solution. The stronger donor properties of 6-Mes, in comparison with other NHCs, were revealed in solution by significant shift of carbene carbon in ^{13}C NMR upon coordination of 6-Mes to Ga and In of $Me_2MOR(6\text{-Mes})$ (M = Ga, In) and $Me_3In(6\text{-Mes})$. However, in light of other results, including X-ray analysis, they could not indicate the presence of a stronger M–$C_{6\text{-Mes}}$ bond for investigated complexes in comparison with M–C_{SIMes}, M–C_{IMes}, and M–C_{SIPr} of their $Me_2MOR(NHC)$ (M = Ga, In; NHC = SIMes, IMes) and $Me_3In(NHC)$ (NHC = SIMes, IMes, SIPr) analogues. The formation of In–$C_{6\text{-Mes}}$ bond in the case of dimethylindiumalkoxides was not sufficient in order to stabilize $Me_2InOR(NHC)$ complexes. Finally, the investigation of the reactivity of $Me_2M(OCH(Me)CO_2Me)$ towards 6-Mes, with regard to the structure of propagating $Me_2M(OPLA)(6\text{-Mes})$ species in the ROP of *rac*-LA, allowed to clarify the mechanism of the reaction of $Me_2InOR(NHC)$ towards sterically hindered NHCs. With regard to the catalytic activity of $Me_2MOR(NHC)$, the effect of Ga–$C_{6\text{-Mes}}$ and a resulting structure of $Me_2GaOR(NHC)$ influenced mostly stereoselectivity, as well as the extent of transesterification reactions in the polymerization of *rac*-LA, which demonstrated the crucial role of NHC on the catalytic properties of $Me_2GaOR(NHC)$. The mechanism of the ROP of *rac*-LA was in line with the insertion of *rac*-LA into Ga–$O_{alkoxide}$ bond, although the insertion into Ga–$C_{6\text{-Mes}}$ could not be excluded. As a result of even weaker In–$C_{6\text{-Mes}}$ bond in comparison to other In–C_{NHCs} in $Me_2InOR(NHC)$ the insertion of *rac*-LA into In–$C_{6\text{-Mes}}$ occurred and was not surprising in the light of the polymerization of *rac*-LA with previously described by us $Me_2InOR(NHC)$ (NHC = SIMes, IMes). Importantly, the reported studies, concerning both the structure and catalytic activity of $Me_2MOR(6\text{-Mes})$, revealed the effect of the character of M–C_{NHC}, rather than only its strength, which is the subject of our current research.

Supplementary Materials: The following are available online at www.mdpi.com/2304-6740/6/1/28/s1. Figures S1–S58 (including mainly NMR spectra of gallium and indium complexes, NMR data of PLA obtained with selected indium and gallium complexes, NMR spectra of experiments of **1** with 10 eq rac-LA, MALDI-TOF of PLA obtained with **1** and weak interactions within crystal structures of **3** and **4**), cif and cif-checked files.

Acknowledgments: This work was financially supported by the National Science Centre of Poland (SONATA BIS2 Programme, Grant No. DEC-2012/07/E/ST5/02860) and partially supported by Warsaw University of Technology. The authors thank Ireneusz Wielgus from Warsaw University of Technology for MALDI-TOF measurements, Łukasz Dobrzycki from University of Warsaw for help with X-ray measurements and Janusz Zachara from Warsaw University of Technology for helpful discussions.

Author Contributions: Martyna Cybularczyk-Cecotka and Paweł Horeglad conceived and designed the experiments; Martyna Cybularczyk-Cecotka and Anna Maria Dąbrowska performed the experiments; Piotr Guńka was responsible for X-ray measurements; Martyna Cybularczyk-Cecotka, Anna Maria Dąbrowska and Paweł Horeglad analyzed the data and wrote the paper.

Conflicts of Interest: The authors declare no conflict of interest.

References

1. Horeglad, P.; Szczepaniak, G.; Dranka, M.; Zachara, J. The first facile stereoselectivity switch in the polymerization of *rac*-lactide—From heteroselective to isoselective dialkylgallium alkoxides with the help of *N*-heterocyclic carbenes. *Chem. Commun.* **2012**, *48*, 1171–1173. [CrossRef] [PubMed]
2. Horeglad, P.; Cybularczyk, M.; Trzaskowski, B.; Żukowska, G.Z.; Dranka, M.; Zachara, J. Dialkylgallium Alkoxides Stabilized with *N*-Heterocyclic Carbenes: Opportunities and Limitations for the Controlled and Stereoselective Polymerization of *rac*-Lactide. *Organometallics* **2015**, *34*, 3480–3496. [CrossRef]
3. Cybularczyk, M.; Dranka, M.; Zachara, J.; Horeglad, P. Effect of In–C_{NHC} Bonds on the Synthesis, Structure and Reactivity of Dialkylindium Alkoxides: How Indium Compares to Gallium. *Organometallics* **2016**, *35*, 3311–3322. [CrossRef]
4. Fliedel, C.; Schnee, G.; Avilés, T.; Dagorne, S. Group 13 metal (Al, Ga, In, Tl) complexes supported by heteroatom-bonded carbene ligands. *Coord. Chem. Rev.* **2014**, *275*, 63–86. [CrossRef]

5. Osten, K.M.; Mehrkhodavandi, P. Indium Catalysts for Ring Opening Polymerization: Exploring the Importance of Catalyst Aggregation. *Acc. Chem. Res.* **2017**, *50*, 2861–2869. [CrossRef] [PubMed]
6. Myers, D.; White, A.J.P.; Forsyth, C.M.; Williams, C.K. Phosphasalen Indium Complexes Showing High Rates and Isoselectivities in *rac*-Lactide Polymerizations. *Angew. Chem. Int. Ed.* **2017**, *56*, 5277–5282. [CrossRef] [PubMed]
7. Aluthge, D.C.; Ahn, J.M.; Mehrkhodavandi, P. Overcoming aggregation in indium salen catalysts for isoselective lactide polymerization. *Chem. Sci.* **2015**, *6*, 5284–5292. [CrossRef]
8. Normand, M.; Dorcet, V.; Kirillov, E.; Carpentier, J.-F. {Phenoxy-imine}aluminum versus -indium Complexes for the Immortal ROP of Lactide: Different Stereocontrol, Different Mechanisms. *Organometallics* **2013**, *32*, 1694–1709. [CrossRef]
9. Horeglad, P.; Litwińska, A.; Żukowska, G.Z.; Kubicki, D.; Szczepaniak, G.; Dranka, M.; Zachara, J. The influence of organosuperbases on the structure and activity of dialkylgallium alkoxides in the polymerization of *rac*-Lactide: The road to stereo diblock PLA copolymers. *Appl. Organometal. Chem.* **2013**, *27*, 328–336. [CrossRef]
10. Dai, Z.; Sun, Y.; Xiong, J.; Pan, X.; Tang, N.; Wu, J. Simple sodium and potassium phenolates as catalysts for highly isoselective polymerization of *rac*-lactide. *Catal. Sci. Technol.* **2016**, *6*, 515–520. [CrossRef]
11. Bakewell, C.; White, A.J.P.; Long, N.J.; Williams, C.K. Scandium and Yttrium Phosphasalen Complexes as Initiators for Ring-Opening Polymerization of Cyclic Esters. *Inorg. Chem.* **2015**, *54*, 2204–2212. [CrossRef] [PubMed]
12. Abbina, S.; Du, G. Zinc-Catalyzed Highly Isoselective Ring Opening Polymerization of *rac*-Lactide. *ACS Macro Lett.* **2014**, *3*, 689–692. [CrossRef] [PubMed]
13. Arnold, P.L.; Buffet, J.-C.; Blaudeck, R.P.; Sujecki, S.; Blake, A.J.; Wilson, C. C_3-Symmetric Lanthanide Tris(alkoxide) Complexes Formed by Preferential Complexation and Their Stereoselective Polymerization of *rac*-Lactide. *Angew. Chem., Int. Ed.* **2008**, *47*, 6033–6036. [CrossRef] [PubMed]
14. Jensen, T.R.; Breyfogle, L.E.; Hillmyer, M.A.; Tolman, W.B. Stereoelective polymerization of D,L-lactide using *N*-heterocyclic carbene based compounds. *Chem. Commun.* **2004**, 2504–2505. [CrossRef] [PubMed]
15. Jensen, T.R.; Schaller, C.P.; Hillmyer, M.A.; Tolman, W.B. Zinc *N*-heterocyclic carbene complexes and their polymerization of D,L-lactide. *J. Organomet. Chem.* **2005**, *690*, 5881–5891. [CrossRef]
16. Arnold, P.L.; Casely, I.J.; Turner, Z.R.; Bellabarba, R.; Tooze, R.B. Magnesium and zinc complexes of functionalised, saturated *N*-heterocyclic Carbene ligands: carbene lability and functionalisation, and lactide polymerisation catalysis. *Dalton Trans.* **2009**, 7236–7247. [CrossRef] [PubMed]
17. Romain, C.; Fliedel, C.; Bellemin-Laponnaz, S.; Dagorne, S. NHC Bis-Phenolate Aluminum Chelates: Synthesis, Structure, and Use in Lactide and Trimethylene Carbonate Polymerization. *Organometallics* **2014**, *33*, 5730–5739. [CrossRef]
18. Zhao, N.; Hou, G.; Deng, X.; Zi, G.; Walter, M.D. Group 4 metal complexes with new chiral pincer NHC-ligands: Synthesis, structureand catalytic activity. *Dalton Trans.* **2014**, *43*, 8261–8272. [CrossRef] [PubMed]
19. Romain, C.; Heinrich, B.; Bellemin-Laponnaz, S.; Dagorne, S. A robust zirconium *N*-heterocyclic carbene complex for the living and highly stereoselective ring-opening polymerization of *rac*-lactide. *Chem. Commun.* **2012**, *48*, 2213–2215. [CrossRef] [PubMed]
20. Romain, C.; Brelot, L.; Bellemin-Laponnaz, S.; Dagorne, S. Synthesis and Structural Characterization of a Novel Family of Titanium Complexes Bearing a Tridentate Bis-phenolate-*N*-heterocyclic Carbene Dianionic Ligand and Their Use in the Controlled ROP of *rac*-Lactide. *Organometallics* **2010**, *29*, 1191–1198. [CrossRef]
21. Schnee, G.; Bolley, A.; Hild, F.; Specklin, D.; Dagorne, S. Group 13 metal (Al, Ga, In) alkyls supported by *N*-heterocyclic carbenes for use in lactide ring-opening polymerization catalysis. *Catal. Today* **2017**, *289*, 204–210. [CrossRef]
22. Patel, D.; Liddle, S.T.; Mungur, S.A.; Rodden, M.; Blake, A.J.; Arnold, P. Bifunctional yttrium(III) and titanium(IV) NHC catalysts for lactide polymerisation. *Chem. Commun.* **2006**, 1124–1126. [CrossRef] [PubMed]
23. Wu, M.M.; Gill, A.M.; Yunpeng, L.; Yongxin, L.; Ganguly, R.; Falivene, L.; Garcia, F. Aryl-NHC-group 13 trimethyl complexes: Structural, stability and bonding insights. *Dalton Trans.* **2017**, *46*, 854–864. [CrossRef] [PubMed]
24. Iglesias, M.; Beetstra, D.J.; Knight, J.C.; Ooi, L.-L.; Stasch, A.; Coles, S.; Male, L.; Hursthouse, M.B.; Cavell, K.J.; Dervisi, A.; Fallis, I.A. Novel Expanded Ring *N*-Heterocyclic Carbenes: Free Carbenes, Silver Complexes, And Structures. *Organometallics* **2008**, *27*, 3279–3289. [CrossRef]
25. Dröge, T.; Glorius, F. The Measure of All Rings—*N*-Heterocyclic Carbenes. *Angew. Chem. Int. Ed.* **2010**, *49*, 6940–6953. [CrossRef] [PubMed]
26. Bourissou, D.; Guerret, O.; Gabbaï, F.P.; Bertrand, G. Stable Carbenes. *Chem. Rev.* **2000**, *100*, 39–91. [CrossRef] [PubMed]

27. Chitsaz, S.; Neumüller, B.Z. Compounds with Organometallic Alkoxo–Indium Cages. *Anorg. Allg. Chem.* **2001**, *627*, 2451–2459. [CrossRef]
28. Chitsaz, S.; Iravani, E.; Neumüller, B.Z. Sesquialkoxides of Gallium and Indium. *Anorg. Allg. Chem.* **2002**, *628*, 2279–2285. [CrossRef]
29. Brown, I.D.; Altermatt, D. Bond-valence parameters obtained from a systematic analysis of the Inorganic Crystal Structure Database. *Acta Crystallogr. Sect. B Struct. Sci.* **1985**, *41*, 244–247. [CrossRef]
30. Kaupp, M.; Metz, B.; Stoll, H. Breakdown of Bond Length-Bond Strength Correlation: A Case Study. *Angew. Chem. Int. Ed.* **2000**, *39*, 4607–4609. [CrossRef]
31. Higelin, A.; Keller, S.; Göhringer, C.; Jones, C.; Krossing, I. Unusual Tilted Carbene Coordination in Carbene Complexes of Gallium(I) and Indium(I). *Angew. Chem. Int. Ed.* **2013**, *52*, 4941–4944. [CrossRef] [PubMed]
32. Arnold, P.L.; Liddle, S.T. f-block *N*-heterocyclic carbene complexes. *Chem. Commun.* **2006**, 3959–3971. [CrossRef] [PubMed]
33. Horeglad, P.; Ablialimov, O.; Szczepaniak, G.; Dąbrowska, A.M.; Dranka, M.; Zachara, J. Dialkylgallium Complexes with Alkoxide and Aryloxide Ligands Possessing *N*-Heterocyclic Carbene Functionalities: Synthesis and Structure. *Organometallics* **2014**, *33*, 100–111. [CrossRef]
34. Dąbrowska, A.M.; Hurko, A.; Dranka, M.; Varga, V.; Urbańczyk, M.; Horeglad, P. Towards NHC stabilized alkylgallium alkoxide/aryloxide cations—The advances, the limitations and the challenges. *J. Organomet. Chem.* **2017**, *840*, 63–69. [CrossRef]
35. Horeglad, P.; Kruk, P.; Pécaut, J. Heteroselective Polymerization of *rac*-Lactide in the Presenceof Dialkylgallium Alkoxides: The Effect of Lewis Base on Polymerization Stereoselectivity. *Organometallics* **2010**, *29*, 3729–3734. [CrossRef]
36. Lewiński, J.; Horeglad, P.; Wójcik, K.; Justyniak, I. Chelation Effect in Polymerization of Cyclic Esters by Metal Alkoxides: Structure Characterization of the Intermediate Formed by Primary Insertion of Lactide into the Al–OR Bond of an Organometallic Initiator. *Organometallics* **2005**, *24*, 4588–4593. [CrossRef]
37. Dagorne, S.; Le Bideau, F.; Welter, R.; Bellemin-Laponnaz, S.; Maisse-François, A. Well-Defined Cationic Alkyl- and Alkoxide-Aluminum Complexes and Their Reactivity with ε-Caprolactone and Lactides. *Chem. Eur. J.* **2007**, *13*, 3202–3217. [CrossRef] [PubMed]
38. Kolychev, E.L.; Asachenko, A.F.; Dzhevakov, P.B.; Bush, A.A.; Shuntikov, V.V.; Khrustalev, V.N.; Nechaev, M.S. Expanded ring diaminocarbene palladium complexes: synthesis, structure, and Suzuki–Miyaura cross-coupling of heteroaryl chlorides in water. *Dalton Trans.* **2013**, *42*, 6859–6866. [CrossRef] [PubMed]
39. *CRYSALIS^{PRO} Software System*, version 1.171.38.43 (**1**–**3** and (6-Mes)=CH_2) and 1.171.38.46 (**4**); Agilent Technologies: Oxford, UK, 2015.
40. Sheldrick, G.M. Crystal structure refinement with SHELXL. *Acta Crystallogr. Sect. A Found. Adv.* **2015**, *71*, 3–8. [CrossRef] [PubMed]
41. Dolomanov, O.V.; Bourhis, L.J.; Gildea, R.J.; Howard, J.A.K.; Puschmann, H. OLEX2: A complete structure solution, refinement and analysis program. *J. Appl. Crystallogr.* **2009**, *42*, 339–341. [CrossRef]